Distorted wave eikonal approximation calculation of elastic and inelastic differential cross sections in c.m. and lab frames for 40Ca nuclei

Rasha J. Kadhim

College of medicine, University of Sumer, Nasiriyah, Iraq, rashaalwan8080@gmail.com

Hanaa H. Kadhim

College of medicine, University of Sumer, Nasiriyah, Iraq, hanaahasan062@gmail.com

Talib F. Hassen

College of medicine, University of Sumer, Nasiriyah, Iraq, talebalzamili@yahoo.com

Abstract

Calculations have been made for elastic and inelastic differential cross sections of neutron scattering on nuclei near stability (N≥Z) such as 40Ca at energies 12,14,17 and 20MeV, at angles distributed between 20o and 180o. In this study, we applied Distorted Wave Eikonal Approximation for 40Ca nuclei using optical model of wood Saxon potential in two frames: center of mass and laboratory. Comparisons between the cross section estimated in the current work and the empirical data available demonstrate good approximation.

Keywords: *angular distribution; eikonal; elastic scattering; inelastic scattering; optical.*

1. INTRODUCTION

A few isotopes are referred to as "magic" in nuclear physics due to the fact that they have just the proper number of neutrons or protons for forming a complete shell. 2, 8, 20, 28, and 50 are the first few magic numbers. The most prevalent form of calcium, calcium-40, is referred to as "doubly magic" due to its nucleus contains both 20 neutrons and 20 protons. This isotope is particularly stable. Different shapes of the nucleus might have extremely comparable energies in magic nuclei, allowing for coexistence. This illustrates the simultaneous quantum superposition of several neutrons and protons conformations. The process by which a nucleus in the "super deformed" conformation, which resembles a long rugby ball, into the lowest-energy spherical shape is still mostly unknown [1].

Present the microscopic study of the elastic and inelastic neutron scattering data utilizing calcium isotope (40Ca) over energies (12,14,17,20 MeV). This paper describes the analysis of the optical model of this target. For input parameters, the parameter input reference (RIPL-3 library) has been used. This data was used in both imaginary and real parts of potential visual model, with particular emphasis, in this study, on the theoretical dependence regarding the optical model's capabilities.

For electron-atom scattering in intermediate energy range, Joachain, Chen, and Watson [2] initially proposed eikonal distorted wave Born approximation (DWBA). The fundamental component of this approach is a factor of correction that is applied to the Born approximation's total wave function. Similar to

how multistate impact parameter approach handles it, this factor permits distortion of outgoing as well as incoming wave functions. Yet, multi-state impact parameter technique only produces total cross sections, whereas the Eikonal DWBA gives differential cross sections [3]. Even though various intriguing aspects of such nuclei were inferred in these studies, the examination of momentum distributions, reaction cross sections, and elastic scattering only offers a highly limited access to information on interior structure of such nuclei [4]. Studying inelastic excitation cross sections can be considered as a logical next step in the quest to learn more about nuclei outside of the stability line. In actuality, photonuclear and electron scattering investigations are complemented by Coulomb and nuclear excitations in the nucleus-nucleus scattering, which can be considered as well-established instruments for stable nuclei spectroscopy [5]. With the use of Eikonal approximation, the neutron differential cross-sections of the elastic scattering were computed, and results have been compared to the experimental information received from EXFOR library. In addition to calculating differential cross sections for inelastic scattering, these outcomes were contrasted at various energies.

2. Eikonal approximation

The DWBA amplitude of transition for reaction A(a, b)B includes matrix element of following form:

$$T_{DWBA} = \int \psi_\beta^{(-)}(r)\langle b, B|U_{int}(r)|a, A\rangle \psi_\alpha^{(+)}(r)d^3r_\alpha d^3r_\beta \qquad (1)$$

$U_{int}(r)$ represents interaction potential, and Ψ_α (Ψ_β) represents scattering wave function in a channel of the entrance (or the exit), $\alpha = a+A$ ($\beta = b+B$). ha, A| and h$_b$, B| represent initial and final intrinsic system wave functions. Utilizing eikonal approximations for the wave functions we can have [6]:

$$\Psi^{(-)*}(r)\Psi^{(+)}(r) \approx \exp\{i\mathbf{q}.\mathbf{r} + i\chi(b)\} \qquad (2)$$

$\chi(b)$ represents eikonal phase which has been expressed as:

$$\chi(b) = -\frac{1}{\hbar v}\int_{-\infty}^{\infty}dz\, U_{opt}(r) \qquad (3)$$

eikonal approximation validity conditions include: (a) forward scattering, in other words, $\theta \ll 1$ radian, (b) small energy is transferred from the bombarding energy to projectile, or target's internal freedom degrees. Those two conditions perfectly apply to the direct processes in the nuclear scattering at $E_{lab} \geq$ 50MeV for each one of the nucleons.

In the equation that has been presented above, $U_{opt}(r)$ represents optical potential, with $r = \sqrt{= b^2 + z^2}$, where b may be interpreted as parameter of impact. For Coulomb part of the optical potential such integral will diverge. One solves that with the use of the equation $\chi = \chi_C + \chi_N$ [7] where χ_N has been given by the eq. above with no Coulomb potential and writing Coulomb eikonal phase, χ_C in the following form:

$$\chi_C(b) = 2\eta\, \ln(kb) \qquad (4)$$

$\eta = Z_1 Z_2 e^2/\hbar v$, Z_1 & Z_2 represent projectile and target charges, v represents the relative velocity, k represents their wave-number in mass system center. Eq4 re-produces the precise amplitude of the Coulomb scattering in the case where it is utilized in calculating elastic scattering with eikonal approximations [8]

$$f_c(\theta) = \frac{z_1 z_2 e^2}{2\mu v^2 \sin^2(\theta/2)} \exp\{-i\eta \ln[\sin^2(\theta/2) + i\pi + 2i\phi_0]\} \tag{5}$$

where $\phi_0 = \arg\Gamma(1+i\eta/2)$.

3. The optical potential.

Optical potential that has been utilized in the calculation processes is described as Woods–Saxon potential as:

$U_{opt} = -V_0 f(r,R_r,a_r) - iW_0 f(r,R_i,a_i)$ (6)

$f(r,R,a) = 1/\{1 + \exp[(r - R)/a]\}^{-1}$.

Parameters that enter those potentials have been fitted for reproduction of data of elastic scattering   [8].
The radii of the colliding system are:

$$R_{r(i)} = r_0(A_p^{1/3} + A_t^{1/3})$$

where V_0, W_0, $R_{r(i)}$ and $a_{r(i)}$ are real and imaginary part of optical potential, real and imaginary radii parameters in fm, and real and the imaginary parameters of diffuseness in fermi. A_P & A_t are projectile number and target mass number.

$$\frac{d\sigma_{el}}{d\Omega} = |f_{el}(\theta)|^2.$$

4. Elastic scattering

In the cases of the nucleus-nucleus collision, the elastic scattering represents a well-known method for examining ground state density values. which has been found to be due to the

$$f_{el}(\theta) = f_C(\theta) + ik \int_0^\infty db\, b\, J_0(qb) \exp[i\chi_C(b)]\{1 - \exp[i\chi_N(b')]\},$$

fact that by folding nucleon-nucleon interactions with nuclear densities of 2 colliding nuclei, optical potential could be connected to ground state density values. However, as we saw in previous section, such relation isn't simple [9,10]. It is dependent upon the efficient interactions that had been

employed, how polarization effects are handled, and other factors (for a review see, [11]. If multiple nucleon-nucleon scattering effects could be ignored, a direct link between the optical potential and nuclear densities is conceivable at greater bombarding energy values (ELab $\geqslant$ 50MeV per nucleon) [12]. Particularly for radioactive beams with low excitation energies, the results of the real or the imaginary nuclear excitations must be considered.

The calculations of the amplitudes of elastic scattering utilizing the eikonal wave functions, Eq2, is quite simple. They can be expressed as [13]   (7)

$$f_{el}(\theta) = ik \int_0^\infty db\, b\, J_0(qb)\{1 - \exp[i\chi(b)]\}$$

here, q = 2ksin(θ/2), and θ represents angle of scattering. Cross section of the elastic scattering can be given as:

$$\frac{d\sigma_{el}}{d\Omega} = |f_{el}(\theta)|^2. \tag{9}$$

For the numerical purposes, it would be more convenient to take advantage of analytical formula for Coulomb scattering amplitude. Which is why, in the case where one would add and subtract Coulomb amplitude, $f_C(\theta)$ in Eq8, the result will be as follows:

$$f_{el}(\theta) = f_C(\theta) + ik \int_0^\infty db\, b\, J_0(qb) \exp[i\chi_C(b)]\{1 - \exp[i\chi_N(b')]\},$$

(10)

Here, b has been replaced in $\chi N(b)$ by b, which has been represented by Eq9 in order to form

nuclear recoil, as it has been discussed in Section1 end.

$$f_{inel}^{\mu}(\theta) = ik \int_0^\infty db\, b\, J_\mu(qb) e^{i\chi(b)} a_\mu(b),$$

The benefit in the use of that equation is that term (1 - exp[iχN(b)]) will be equal to 0 for the impact parameters which are larger than summation of nuclear radii (i.e. the grazing impact parameter). Which is why, integral must only be carried out within small range. In this equation, χ_C has been represented by Eq4 and $f_C(\theta)$ has been represented by Eq5, with

$$\phi_0 = -\eta C + \sum_{j=0}^{\infty} \left(\frac{\eta}{j+1} - \arctan \frac{\eta}{j+1} \right),$$

(11)

and C = 0.57721560... represents Euler's constant value.

Eqs. (9-11) describes A(projectile) + B's elastic scattering cross section in mass system's center. In the lab, angle of scattering can be expressed as [14]

$\theta_L = \arctan\{ \sin\theta /\gamma \, [\cos\theta + pg(p, E_1)]\}$

, $p = M_A/M_B$

$E1 = E_{lab}[MeV/nucleon]/ m_N c^2$, where m_N is the nucleon mass, and

$$g(\rho, \mathcal{E}_1) = \frac{1 + \rho(1 + \mathcal{E}_1)}{1 + \mathcal{E}_1 + \rho}, \qquad \gamma = \frac{1 + \mathcal{E}_1 + \rho}{\sqrt{(1+\rho)^2 + 2\rho\mathcal{E}_1}}.$$

(12)

γ represent relativistic Lorentz factor of motions regarding center of mass systems in terms of lab.

Lab cross section can be represented as:

$$\frac{d\sigma_{el}}{d\Omega_L}(\theta_L) = \frac{\{\gamma^2[\rho g(\rho, \mathcal{E}_1) + \cos\theta]^2 + \sin^2\theta\}^{3/2}}{\gamma[1 + \rho g(\rho, \mathcal{E}_1)\cos\theta]} \frac{d\sigma_{el}}{d\Omega}(\theta).$$

(13)

5. Angular distribution of the particles scattered inelastically

Angular distribution of particles that are scattered inelastically may be determined by:

$$f_{inel}^{\mu}(\theta) = ik \int_0^\infty db\, b\, J_\mu(qb) e^{i\chi(b)} a_\mu(b),$$

(14)

where we simplified the notation: aμ ≡ a_{InMn},$^M_1$, with μ = $M_n - M_1$.

The mean value over initial spin and the summation over final spin are used to calculate inelastic scattering cross section:

$$\frac{d\sigma_{inel}}{d\Omega} = \frac{1}{2I_1 + 1} \sum_{M_1, M_n} |f_{inel}^{\mu}|^2.$$

(15)

Equation (15) has been used by the DWEIKO program to determine angular distribution in the inelastic scattering. However, it would be useful to see the way that it connects to a typical semi-classical approximation.

6. Results

Optical model potentials (OMP), which are employed by default, were obtained from Koning [15]. Although the low energy boundary of validity might vary from nucleus to nucleus (for the total Cross section), such phenomenological OMPs for neutrons are theoretically valid spanning the (12–20 MeV) energy range. For the 40Ca target, Table 1 shows the results of solving the Schrodinger equation using this OMP: the shape-elastic cross section, total cross section, wave functions for direct reaction cross, shape-elastic angular distribution, and optical modal. Nuclear several radial distances (r), along with imaginary and real potential strength values Wo and Vo have been found effective for the global potential parameters [9], yet in this

computation, they were diverted and a and r were maintained fixed as in Table1.

Table1. optical potential Parameters utilized in the calculation of the angular distribution from Koning [9].

E_{in} MeV	V_v MeV	r_v fm	a_v fm	W_v MeV	r_{wv} fm	a_{wv} fm	W_s MeV	r_{ws} fm	a_s fm	V_{so} MeV	r_{so} fm	a_{so} fm
12	49.6	1.21	0.68	1.1	1.21	0.68	6.7	1.29	0.54	5.5	1.01	0.60
14	48.9	1.21	0.68	1.3	1.21	0.68	6.7	1.29	0.54	5.5	1.01	0.60
17	47.8	1.21	0.68	1.6	1.21	0.68	6.5	1.29	0.54	5.4	1.01	0.60
20	46.7	1.21	0.68	1.9	1.21	0.68	6.4	1.29	0.54	5.4	1.01	0.60

The main results of the excited nuclei are $< r2>$ = 11.948 with root mean square$< r2 >1/2 =$ 3.457for energies 10,12,14,17 and 20 MeV, respectively[15,16]. Gamma or Lorentz factor (1.013.1.015, 1.018, 1.021) wavenumber (k)=0.741, 0.801, 0.883, 0.959 and Somerfield parameter for all energies is zero due to the fact that the charge of neutron is zero. Total nuclear reactions cross section = -7589.40, -5738.37, -3710.27, -2624.02 mb for 12,14,17 and 20 MeV, respectively. The excitation cross-sections for nucleus from state to state are tabulated in Table 2.

Table (2) Excitation cross section in unite of (mb) for incident neutrons with energies12,14, 17 and 20MeV

Energy	12MeV	14MeV	17MeV	20MeV
State 2	0.357E+04	0.269E+04	0.184E+04	0.142E+04
State 3	0.616E-01	0.479E-01	0.327E-01	0.245E-01
The total	0.357E+04	0.269E+04	0.184E+04	0.142E+04

In the present work, we have performed elastic scattering cross section for different neutron projectile incident energies (12, 14, 17, and 20 MeV) in two frames (laboratory and c.m.) through subtracting non-elastic cross section from overall cross section to 40Ca isotope, as seen in fig. (1)

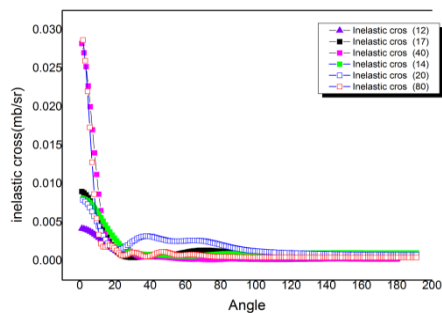**Figure1(a, b) elastic cross section in laboratory system and center of mass**
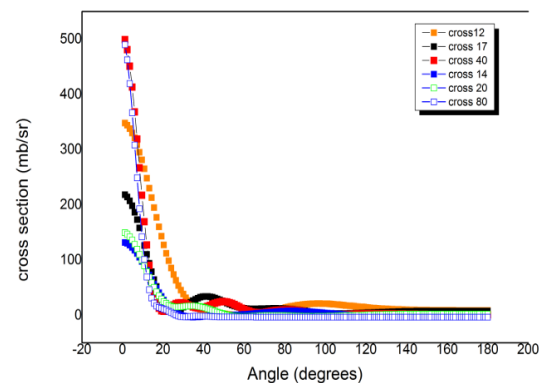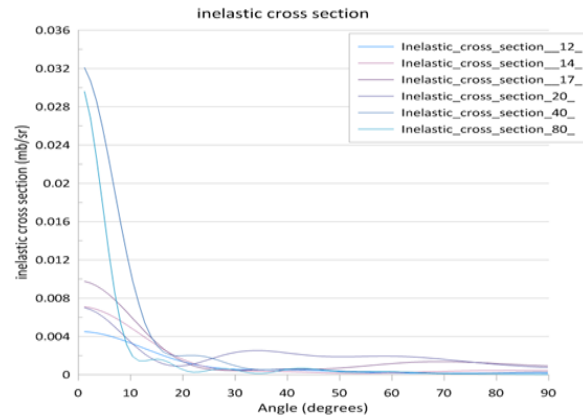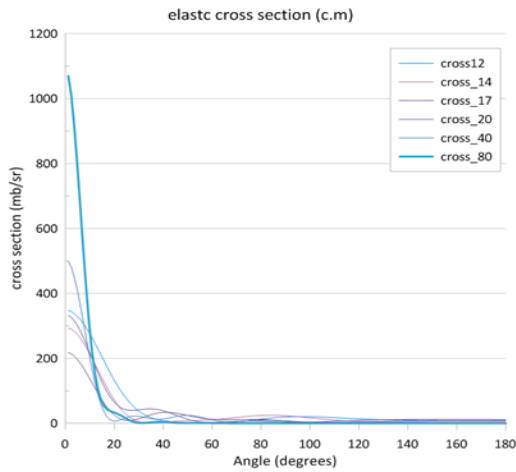
By considering coupled channels between 2 target states and assuming that the projectile being employed is a spherical neutron and the target is a deformed nucleus (40Ca), the analysis of inelastic differential cross-section was completed. The parameter of the deformation $\beta\lambda$ (are ($\beta2= 0.731$, $\beta3 = 0.36$) fm) that correspond to the states of energies of the excitation of the low lying states of vibration 2+ and 3+ (E2= 10.9MeV, E3=13.5 MeV) comparing with experimental one for E2= 11.9 MeV[18]. Figures 2 and 3 show that the behavior regarding such two frames, C.M. and lab, behaved similarly with just minor changes during the measurements.

Figure 2 (a, b) inelastic cross section in c. m and laboratory system.

At comparison to practical differential elastic cross sections, computed differential cross-section for elastic n+40Ca scattering at specific energy values in center of mass (c.m.) is shown in Figures (3,4). The red dots reflect the experimental data, whereas solid line represents estimated differential cross section. Figures 3 and 4 show that the neutron's Eikonal model results in well-defined angle dependency for both experimental and calculated data. For every energy at different angle, experimental data cross-section flexures significantly. The goal of this is to account for measurement uncertainties that are present in experimental data, yet not in the theoretical calculations. According to the conclusions of the Eikonal model, the cross-section should be smaller for larger angles and higher for smaller angles.
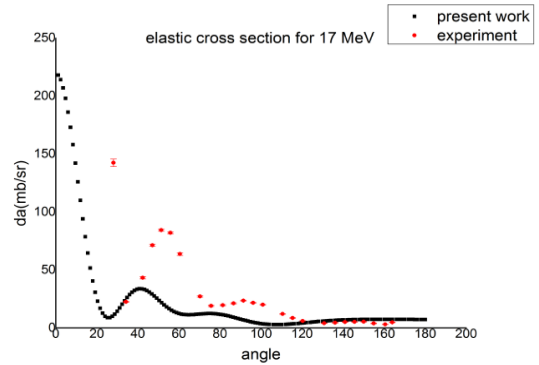
Figure 3 (a,b) comparison of elastic cross section for 12,14 MeV neutron energy of present work and available experiment data[15,16].
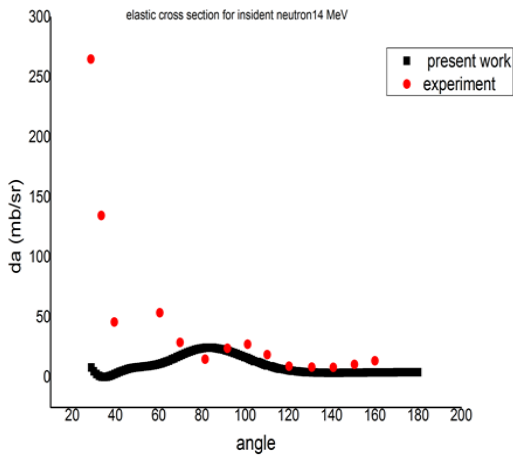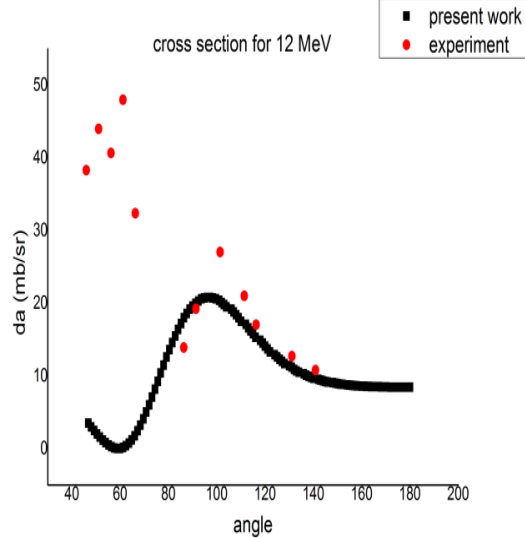
Figure (4) Comparison regarding elastic cross section for 17 MeV neutron energy of present study as well as experiment data[19].

Both the imaginary and real parts regarding an effective potential have been plotted, as seen in Figure 5, to see how first-order Eikonal modification affected the effective potential. The colored solid curves in this figure represent the effective potential Ueff (r). The two potentials differ significantly, as shown in the Figure, particularly in small r regions. The terms of correction holding the product of imaginary and real potentials as well as their derivatives are what cause the effective potential to change dramatically. In imaginary potential rather than real potential, the degree of change is more apparent. As seen in Figure 5(b), the nominal real potential rises monotonically, whereas the effective imaginary potential pronounced minimum about r = 5fm and after that increases. Surface region of colliding nuclei plays a significant role in differential cross-section, hence the discrepancy in r region (1-4) fm is not substantial.

Figure 5 (a, b) Imaginary and real optical potentials that have been utilized in optical model analysis of various energy values (MeV) for the elastic scattering.
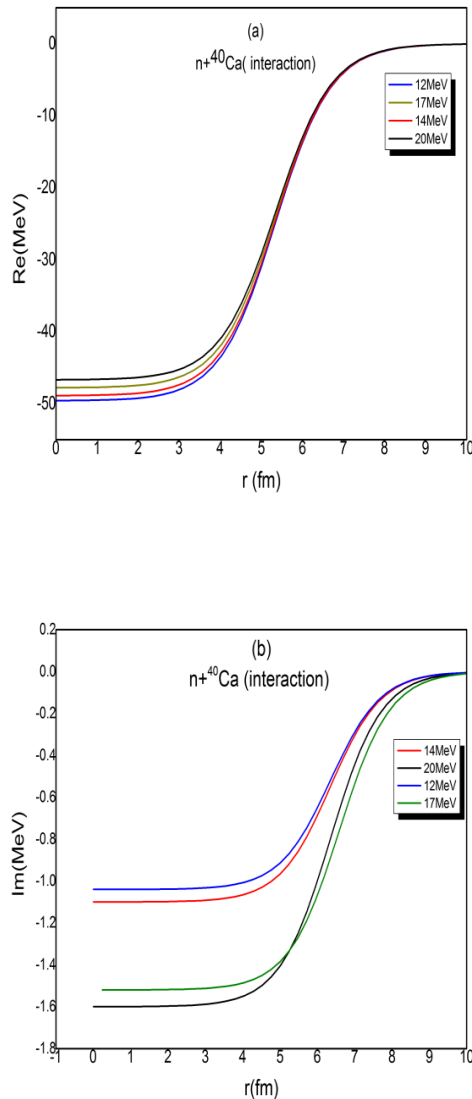
current cross section. The excitation energy range of interest in 40Ca has nuclear structural effects that impede a complete explanation of the data at all energies. A fair description of differential cross section in the neutron-calcium scattering was accomplished over entire energy range that has been analyzed, according to outcomes when compared to n+40Ca scattering and experiment data.

Reference

[1] E. Ideguchi et al., "Electric Monopole Transition from the Superdeformed Band in $^{40}\mathrm{Ca}$," Phys. Rev. Lett., vol. 128, no. 25, p. 252501, 2022, doi: 10.1103/PhysRevLett.128.252501.

[2] J. C. Y. Chen, C. J. Joachain, and K. M. Watson, "Eikonal Theory of Inelastic Electron-Atom Scattering at Intermediate Energies," Phys. Rev. A, vol. 5, no. 6, pp. 2460–2474, 1972, doi: 10.1103/PhysRevA.5.2460.

[3] R. H. Shields and R. H. Shields, "Scholars ' Mine The eikonal distorted wave Born approximation for the excitation of hydrogen by impact with hydrogen and helium in the intermediate energy range by Presented to the Faculty of the Graduate School of the," 1972.

[4] C. A. Bertulani and H. Sagawa, "Probing the ground-state and transition densities of halo nuclei," Nucl. Physics, Sect. A, vol. 588, no. 3, pp. 667–692, 1995, doi: 10.1016/0375-9474(95)00022-S.

[5] K. Planckstr, M. Sciences, and A. Ikki-machi, "Probing the ground state and transition densities of halo nuclei," no. c.

[6] C. A. Bertulani, C. M. Campbell, and T. Glasmacher, "A computer program for nuclear scattering at intermediate and high energies," Comput. Phys. Commun., vol. 152, no. 3, pp. 317–340, 2003, doi:

7. Conclusion

Cross-section measurements for calcium neutrons scattered inelastically and elastically at 12, 14, 17, and 20 MeV are provided. The data cannot be reproduced by any of global neutron-nucleus optical model parameter sets that are typically cited in literature, particularly

https://doi.org/10.1016/S0010-4655(02)00824-X.

[7] A. N. F. Aleixo, "Nucleon-nucleon correlation effects in the elastic scattering ofa particles from "Li at 26 MeV/nucleon," Phys. Rev. C, vol. 45, no. 5, 1992.

[8] G. M. C.A. Bertulani, M.S. Hussein, Physics of Radioactive Beams. Huntington, New York: Nova Science, 2002.

[9] G. R. Satchler, Direct nuclear reactions. Oxford; New York: Clarendon Press ; Oxford University Press, 1983.

[10] C. A. Bertulani, P. Danielewicz, and E. Lansing, Introduction to Nuclear Reactions. East Lansing: Taylor & Francis Group, 2003.

[11] M. S. Hussein, R. A. Rego, and C. A. Bertulani, "Microscopic theory of the total reaction cross section and application to stable and exotic nuclei," Phys. Rep., vol. 201, no. 5, pp. 279–334, 1991, doi: https://doi.org/10.1016/0370-1573(91)90037-M.

[12] A. K. Kerman, H. McManus, and R. M. Thaler, "The scattering of fast nucleons from nuclei," Ann. Phys. (N. Y)., vol. 8, no. 4, pp. 551–635, 1959, doi: https://doi.org/10.1016/0003-4916(59)90076-4.

[13] R.J. Glauber, "High-energy collisions theory, in: Lectures in Theoretical Physics, Interscience," New York, 1959.

[14] Herbert Goldstein, "Classical_Mechanics." Addison-Wesley Publishing Company, New York, 1980.

[15] A. J. Koning and J. P. Delaroche, "Local and global nucleon optical models from 1 keV to 200 MeV," Nucl. Phys. A, vol. 713, no. 3, pp. 231–310, 2003, doi:

https://doi.org/10.1016/S0375-9474(02)01321-0.

[16] Naz.t.jarallah, "Study The Deformation Parameters (β 2, δ) For Even - Even," J. Coll. Educ., pp. 189–200, 2016.

[17] B. S. Ishkhanov, M. E. Stepanov, and T. Y. Tretyakova, "Nuclear spectroscopy of 40–48Ca isotopes," Moscow Univ. Phys. Bull., vol. 69, no. 6, pp. 433–456, 2014, doi: 10.3103/S0027134914060095.

[18] S. Raman, C. W. Nestor, and P. Tikkanen, "Transition probability from the ground to the first-excited 2+ state of even-even nuclides," At. Data Nucl. Data Tables, vol. 78, no. 1, pp. 1–128, 2001, doi: 10.1006/adnd.2001.0858.

[19] J. M. Mueller et al., "Asymmetry dependence of nucleon correlations in spherical nuclei extracted from a dispersive-optical-model analysis," Phys. Rev. C - Nucl. Phys., vol. 83, no. 6, pp. 1–32, 2011, doi: 10.1103/PhysRevC.83.064605.

[20] W. Tornow et al., "Analyzing power and differential cross section at 9.9, 11.9 and 13.9 MeV for Ca(n, n)Ca," Nucl. Phys. A, vol. 385, no. 3, pp. 373–406, 1982, doi: https://doi.org/10.1016/0375-9474(82)90093-8.